Description of Stress-Controlled Cyclic Plasticity Using the Cyclic Nonhardening Region Model

N. Ohno, Y. Kachi

Toyohashi University of Technology, Dept. of Energy Engineering, Tempaku-cho, Toyohashi 440, Japan

Abstract

A constitutive model based on the concept of a cyclic nonhardening region is used to describe cyclic plastic behaviours of 304 stainless steel under stress- and strain-controlled cyclic loadings: With a set of material constants determined from some strain-controlled experimental results, predictions of the model are calculated for several kinds of stress- and strain-controlled cyclic loadings, and compared with the corresponding experimental results. It is shown that the model describes fairly accurately the cyclic plastic behaviours of 304 stainless steel under these loading conditions at room temperature, and that cyclic stress-strain curves calculated under the conditions of constant strain- and stress-ranges coincide with each other, as observed in the experimental results. A limitation of the model is also discussed that, in the case of stress-controlled cyclic loadings, predicted mean-strains may differ largely from experimental ones.

1. Introduction

Let us consider structural analysis of a component, with areas of stress concentration, subjected to cyclic loading. Distributions of stress and strain are nonuniform in the component. Therefore, a constitutive model of cyclic plasticity used in the analysis must be valid for any magnitude of cyclic stress- or strain-range occurring in the component. Moreover, material elements in the areas of stress concentration may be subjected to cyclic loadings in which stress- and strain-controlled ones are mixed. For example, in the case of cyclic hardening materials, as cyclic hardening proceeds, the increase of stress amplitude and the decrease of strain one may occur simultaneously there. Therefore, it is necessary to examine the validity of the constitutive model under both stress- and strain-controlled conditions.

Constitutive models of cyclic plasticity were proposed by introducing the concept of a cyclic nonhardening region in plastic strain space [1, 2]. Although the model in [1] is limited to linear hardening materials in effect, it was improved in [2] to describe nonlinear hardening of materials. They will be reviewed briefly later. It was shown that the nonlinear hardening model successfully simulates the experimental results of 304 and 316 stainless steels under several levels of strain-controlled cyclic loadings [2]. However, its validity has not been examined yet under stress-controlled cyclic loadings.

In the present paper, by use of the nonlinear hardening model mentioned above, cyclic

plastic behaviours are calculated for several kinds of stress- and strain-controlled cyclic loadings, and calculated results are compared with experimental results of 304 stainless steel at room temperature. Only a set of material constants is used. Thus, the validity of the model is discussed in both cases of stress- and strain-controlled cyclic loadings.

2. Constitutive Model

Let us briefly review the linear [1] and nonlinear [2] hardening models in the case of uniaxial loading of stress σ, strain ε, and plastic strain ε^p. Multiaxial forms of them are found in [1, 2].

2. 1 Cyclic nonhardening range We assume the development of a plastic strain range, called the cyclic nonhardening range, of cener α and size ρ :

$$g = (\varepsilon^p - \alpha)^2 - \rho^2 \leqq 0 \tag{1}$$

where α and ρ develop as

$$\dot{\alpha} = (1 - c)\Gamma \dot{\varepsilon}^p \tag{2}$$

$$\dot{\rho} = c\Gamma |\dot{\varepsilon}^p| \tag{3}$$

$$\Gamma = \begin{cases} 1, & g = 0 \quad \text{and} \quad (\partial g/\partial \varepsilon^p)\dot{\varepsilon}^p > 0 \\ 0, & g < 0 \quad \text{or} \quad (\partial g/\partial \varepsilon^p)\dot{\varepsilon}^p \leqq 0 \end{cases} \tag{4}$$

Here and from now on $(\dot{})$ stands for the derivative with respect to a certain loading parameter. It is seen from eqs.(2)-(4) that the expansion and translation of the range $g \leqq 0$ occurs, only when plastic strain point ε^p is located on the bound $g = 0$ and moves outward in plastic strain space.

We postulate that *when pastic strain point* ε^p *moves inside the range* $g \leqq 0$, *neither isotropic hardening nor cyclic hardening of materials is accumulated*, as will be formulated in the following subsections.

Chaboche et al. [3] used first a special case of the range $g \leqq 0$ with $c = 1/2$. Dafalias [11] and Dafalias and Seyed-Ranjbari [12] used the range $g \leqq 0$, too. Murakami and Ohno [4] and Ohno et al. [5] proposed constitutive models of creep with the range $g \leqq 0$.

2. 2 Linear hardening Model Assuming linear isotropic-kinematic hardening of materials, we can consider the following constitutive relations incorporating Γ defined by eq. (4):

$$f = (\sigma - \eta)^2 - \kappa^2 = 0 \tag{5}$$

$$\dot{\eta} = [K + (1 - \Gamma)L]\dot{\varepsilon}^p \tag{6}$$

$$\kappa = \kappa_0 + Lq, \quad \dot{q} = \Gamma |\dot{\varepsilon}^p| \tag{7}$$

$$\dot{\varepsilon}^p = \dot{\sigma}/(K + L) \tag{8}$$

where f is a yield function, η and κ denote the center and size of the elastic stress range, q is an isotropic hardening variable, K and L are material constants expressing hardening of materials, and κ_0 is the initial value of yield stress.

When plastic strain point ε^p is located on the bound $g = 0$ and moves outward ($\Gamma = 1$), eqs. (5)-(8) are reduced to relations for the linear combined hardening model of kinematic hardening modulus K and isotropic one L. On the other hand, when ε^p moves inside the

range $g \leqq 0$ ($\Gamma = 0$), the isotropic hardening variable q does not change, and thus eqs. (5)- (8) express the kinematic hardening model of hardening modulus $K + L$.

Figure 1 shows the changes of the center η and size κ of elastic stress range, together with the development of the cyclic nonhardening range $g \leqq 0$, under tensile loading, unloading and reverse loading. The range $g \leqq 0$ develops continuously under the tensile loading ($\Gamma = 1$), and it occupies $[\varepsilon^p_A, \varepsilon^p_B]$ at the instant of the unloading. Until ε^p reaches ε^p_A under the reverse loading ($\Gamma = 0$), the range $g \leqq 0$ does not develop, and moreover plastic hardening of materials proceeds purely kinematically with kinematic hardening modulus $K + L$. After ε^p reaches ε^p_A ($\Gamma = 1$), the range $g \leqq 0$ and the isotropic hardening variable q develop again.

Once the cyclic nonhardening range develops and covers a cyclic range of plastic strain, Γ always takes the value of zero. Then, cyclic hardening of materials becomes saturated, and the range $g \leqq 0$ ceases to develop, as seen from eqs. (2), (3) and (7).

2. 3 Nonlinear hardening model The linear hardening model by eqs. (5)-(8) can be extended to a nonlinear hardening model, if we adopt a two-surface plasticity model. Namely, a bounding surface inside which a yield surface translates is assumed in order to describe nonlinear hardening of materials [6 - 9], and the concept of a cyclic nonhardening region is applied to specifying evolution equations of the bounding surface.

Let us regard the yield surface in the linear hardening model, eqs. (5)-(7), as a bounding surface:

$$f^* = (\sigma^* - \eta^*)^2 - \kappa^{*2} = 0 \tag{9}$$

$$\dot{\eta}^* = [K + (1 - \Gamma)L]\dot{\varepsilon}^p \tag{10}$$

$$\kappa^* = \kappa^*_0 + Lq\,, \quad \dot{q} = \Gamma|\dot{\varepsilon}^p| \tag{11}$$

where η^* and κ^* denote the center and size of the bounding surface, and κ^*_0 is its initial size.

We assume for simplicity a yield surface of constant size

$$f = (\sigma - \eta)^2 - \kappa^2 = 0\,, \quad \kappa = \kappa_0 \text{ (constant)} \tag{12}$$

which translates inside the bounding surface in a way expressed as

$$\dot{\eta} = A(\sigma^* - \sigma)|\dot{\varepsilon}^p| \tag{13}$$

In eq. (13), A is a constant, and σ^* denotes the stress state taken on the bounding surface to be

$$\sigma^* = \eta^* + \mathrm{sgn}[\sigma - \eta]\,\kappa^* \tag{14}$$

Then, the consistency condition $\dot{f} = 0$ gives

$$\dot{\varepsilon}^p = (1/A)\,\mathrm{sgn}[\sigma - \eta]\,\dot{\sigma}/(\sigma^* - \sigma) \tag{15}$$

As shown in Fig. 2, stress σ approaches to the bounding stress σ^* specified by eqs. (14), (10) and (11), so that nonlinear hardening of materials can be described.

3. Comparison With Experimental Results of 304 Stainless Steel

Only the nonlinear hardening model is discussed in comparison with experimental results

of 304 stainless steel under uniaxial cyclic loadings at room temperature. From now on, symbols $\Delta\sigma$ and $\Delta\varepsilon$ denote the magnitudes of cyclic stress- and strain-ranges, respectively, and R_ε or R_σ stands for the ratio of a lower limit to upper one under strain- or stress-controlled cyclic loading.

3. 1 Strain-controlled tests The material constants in the nonlinear hardening model were determined, as explained in [2], so as to simulate experimental data under strain-controlled conditions, i. e., the monotonic and cyclic curves of stress vs. plastic strain in Fig. 3 and the stress-strain hysteresis loops of constant strain-range in Fig. 4. Thus, we obtained

$$\left.\begin{aligned} &\kappa_0 = 185\ \text{MPa},\quad \kappa^*_0 = 255\ \text{MPa},\quad A = 500 \\ &K = 1456\ \text{MPa},\quad L = 1044\ \text{MPa},\quad c = 0.08 \end{aligned}\right\} \tag{16}$$

Table I shows comparisons between calculated and experimental results under strain-controlled cyclic loadings with and without mean-strain. Good agreement is seen between them. We emphasize that the present model is valid for all the values of $\Delta\varepsilon$ examined here. This feature of the model is important, when structural components with nonuniform strain distributions are analyzed, as mentioned in Introduction. It is also seen that the model describes the experimental tendency that the saturated value of $\Delta\sigma$ depends little on R_ε.

3. 2 Stress-controlled tests Table II shows experimental results and predictions in several cases of stress-controlled cyclic loadings with and without mean-stress. Figures 5 and 6 are examples of comparison between experimental and predicted $\sigma - \varepsilon$ hysteresis loops of stress-control.

First let us discuss the changes of $\Delta\varepsilon$. It can be found from Table II and Figs. 5 and 6 that as regard $\Delta\varepsilon$ the predictions agree with the experimental results fairly accurately. Figure 7 shows the saturated $\Delta\sigma/2 - \Delta\varepsilon/2$ curves calculated under the conditions of constant stress- and strain-ranges, together with the corresponding experimental data. It is seen that these theoretical curves coincide with each other, as observed in the experimental results. This tendency was observed on 316 stainless steel at room temperature, too [10].

The coincidence between the calculated curves in Fig. 7 is explained as follows: The saturation of cyclic hardening occurs, when the cyclic nonhardening range $g \leqq 0$ develops and involves a cyclic range of plastic strain. If the material constant c is small enough as in the present work, the range $g \leqq 0$ develops little by little as the number of cycles increases. Thus, in the saturated state of cyclic hardening, the range $g \leqq 0$ coincides, or nearly coincides, with the cyclic range of plastic strain. Therefore, eqs. (7) and (3) give the saturated value of the isotropic hardening variable q as

$$q_s = (1/c)\rho_s \fallingdotseq (1/c)\Delta\varepsilon^p_s/2 \tag{17}$$

where the subscript s denotes the saturated state of cyclic hardening. Since the above relation holds in both cases of constant cyclic stress- and strain-ranges, the same, or nearly the same, $\Delta\sigma_s - \Delta\varepsilon^p_s$ curve is obtained for these two types of cyclic loadings.

As regards mean-strain ε_{mean}, on the other hand, the predictions differ largely from the experimental results (Table II and Fig. 5). Moreover, although the present model describes racheting of ε_{mean} under nonzero mean-stress, the calculated results do not agree

qualitatively with the experimental results (Table II and Fig. 6). Such disagreement on ε_{mean} causes serious errors, when racheting of ε_{mean} is significant. However, as long as we analyze distributions of cyclic stress- and strain-amplitudes in structural components, it may have little influence.

4. Conclusions

The validity of a nonlinear constitutive model of cyclic plasticity based on the concept of a cyclic nonhardening region was examined under both stress- and strain-controlled conditions. Cyclic plastic behaviours calculated under these loading conditions were compared with experimental results of 304 stainless steel at room temperature. The following conclusions were obtained:

1) For strain-controlled cyclic loadings with and without mean-strain, the model successfully describes the experimental results.

2) For stress-controlled cyclic loadings with and without mean-stress, the predictions agree with the experimental results fairly accurately as regard the magnitude of cyclic strain-range, but not so as regard mean-strain.

3) The cyclic stress-strain curves calculated under the conditions of constant stress- and strain ranges coincide with each other, as observed in the experimental results.

4) The disagreement on mean-strain between calculated and experimental results may restrict the use of the model to cases in which racheting of mean-strain is not significant.

References

[1] Ohno, N., "A Constitutive Model of Cyclic Plasticity With a Nonhardening Strain Region," *ASME J. Appl. Mech.* **49**, 721-727 (1982).

[2] Ohno, N., Kachi, Y., Murakami, S., "A Constitutive Model of Cyclic Plasticity for Nonlinear Hardening Materials," *Preprint of JSME*, No. 840-9, 16-23 (1984), (in Japanese).

[3] Chaboche, J.L., Dang Van, K., Cordier, G., "Modelization of the Strain Memory Effect on the Cyclic Hardening of 316 Stainless Steel," *Proceedings 5th Int. Conf. on Structural Mechanics in Reactor Technology*, Vol. L, 1979, Paper No. L 11/3.

[4] Murakami, S., Ohno, N., "A Constitutive Equation of Creep Based on the Concept of a Creep-Hardening Surface," *Int. J. Solids Structures* **18**, 597-609 (1982).

[5] Ohno, N., Murakami, S., Ueno, T., "A Constitutive Model of Creep Describing Creep Recovery and Material Softening Caused by Stress Reversals," *ASME J. Eng. Mat Tech.* **107**, 1-6 (1985).

[6] Mróz, Z., "An Attempt to Describe the Behavior of Metals Under Cyclic Loads Using a More General Workhardening Model," *Acta Mech.* **7**, 199-212 (1969).

[7] Krieg, R.D., "A Practical Two Surface Plasticity Theory," *ASME J. Appl. Mech.* **42**, 641-646 (1975).

[8] Dafalias, Y.F., Popov, E.P., "A Model of Nonlinearly Hardening Materials for Complex Loading," *Acta Mech.* **21**, 173-192 (1975).

[9] Dafalias, Y.F., Popov, E.P., "Plastic Internal Variables Formalism of Cyclic Plasticity," *ASME J. Appl. Mech.* **43**, 645-651 (1976).

[10] Chaboche, J.L, Kaczmarek, H., Raine, P., "Hardening and Fatigue Damage Interaction in 316 L Steel," *T.P. ONERA*, n° 1980-3.

[11] Dafalias, Y.F., "A Novel Bounding Surface Constitutive Law for the Monotonic and Cyclic Hardening Response of Metals," *Proceedings 6th Int. Conf. on Structural Mechanics in Reactor Technology*, Vol. L, 1981, Paper No. L 3/4.

[12] Dafalias, Y.F., Seyed-Ranjbari, M.S., "Constitutive Modeling of Cyclic Metal Plasticity," *Proceedings 2nd Cairo Univ. Conf. on Current Advances in Mechanical Design and Production*, 1982, 429-438.

Table I Experimental results (upper row) and theoretical results (lower row) under strain-controled cyclic loadings; strain in percent, stress in MPa.

$\Delta\varepsilon$	R_ε	1st		2nd		5th		10th		20th	
		$\Delta\sigma$	σ_{mean}	$\Delta\sigma$	σ_{mean}	$\Delta\sigma$	σ_{mean}	$\Delta\sigma$	σ_{mean}	$\Delta\sigma$	σ_{mean}
0.504	-1.74	458.6	-16.6	478.1	-11.3	487.9	-8.6	491.1	-8.1	488.9	-7.0
		443.8	-13.3	460.5	-2.5	469.3	-1.1	472.4	-1.0	473.0	-0.9
0.976	-1.00	488.5	-7.7	521.6	-2.2	558.8	-1.1	576.3	-1.1		
		511.4	-7.2	541.3	-2.3	575.2	-0.8	589.2	-0.1	591.4	0.0
1.996	-1.14	572.8	-20.7	639.7	-9.6	708.8	-6.9	746.1	-4.3	760.9	-2.2
		558.3	-10.4	619.4	-7.1	708.6	-2.9	745.0	-1.2	751.6	-0.9
0.992	-0.01	547.7	3.3	560.8	3.3	584.8	3.3	601.1	2.8	607.7	3.9
		530.8	4.7	549.3	4.5	579.8	5.8	592.2	6.5	594.7	6.6
2.000	-0.02	592.3	-3.3	645.1	-6.0	701.4	-4.9	738.2	-2.7	748.9	-2.8
		580.3	4.9	633.8	7.4	713.6	11.1	746.2	12.6	752.0	12.9
1.012	0.49	562.2	15.2	575.3	10.9	592.6	7.6	604.5	7.1	608.9	7.1
		552.1	19.6	564.1	18.3	587.2	19.5	596.6	19.9	598.3	19.9
0.512	0.75	499.2	52.5	515.4	43.3	525.2	37.4	525.2	33.0	522.0	30.3
		499.9	46.5	479.8	26.2	477.3	23.9	477.3	23.9	477.3	23.9

Table II Experimental results (upper row) and theoretical results (lower row) under stress-controled cyclic loadings;strain in percent, stress in MPa.

$\Delta\sigma$	R_σ	1st		2nd		5th		10th		20th	
		ε_{max}	ε_{min}	$\Delta\varepsilon$	ε_{mean}	$\Delta\varepsilon$	ε_{mean}	$\Delta\varepsilon$	ε_{mean}	$\Delta\varepsilon$	ε_{mean}
476.8	-1.0	0.396	-0.128	0.452	0.110	0.436	0.102	0.440	0.100	0.451	0.095
		0.376	-0.221	0.562	0.063	0.528	0.041	0.518	0.023	0.516	0.007
541.4	-1.0	1.192	0.060	0.788	0.491	0.716	0.462	0.700	0.442	0.700	0.430
		0.999	-0.281	0.878	0.142	0.767	0.050	0.749	0.013	0.746	0.001
594.0	-1.0	2.112	0.664	1.024	1.266	0.884	1.234	0.864	1.228	0.872	1.232
		2.029	-0.458	1.088	0.075	0.996	0.010	0.988	0.001	0.988	0.0
637.0	-1.0	3.056	1.148	1.236	1.842	1.060	1.798	1.032	1.784	1.052	1.786
		2.899	-0.611	1.290	0.033	1.234	0.001	1.233	0.0	1.233	0.0
546.1	-0.8	2.292	1.524	0.672	0.918	0.624	2.000	0.620	2.034	0.624	2.108
		2.289	1.478	0.779	2.004	0.760	2.146	0.762	2.215	0.762	2.234
455.3	-0.5	2.240	1.836	0.376	2.072	0.368	2.132	0.368	2.192	0.372	2.290
		2.292	1.937	0.356	2.446	0.358	3.043	0.361	3.621	0.364	4.261

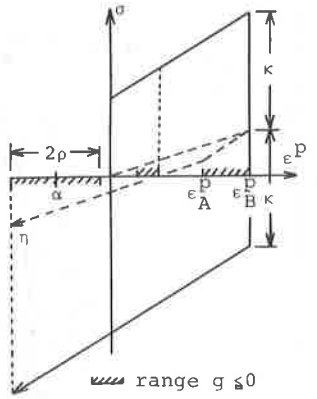

Fig. 1 Stress-strain diagram by linear hardening model.

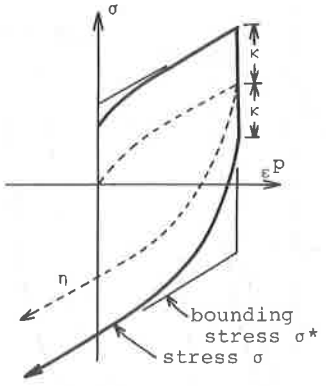

Fig. 2 Stress-strain diagrm by nonlinear hardening model.

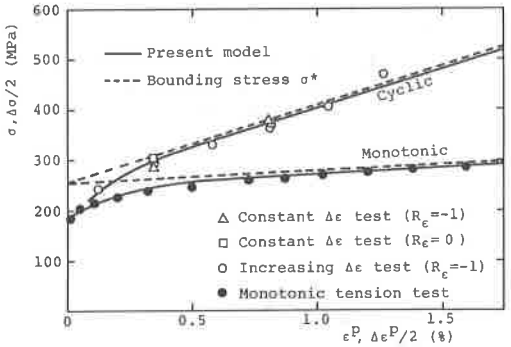

Fig. 3 Monotonic σ-ε^p curve and strain-controlled $\Delta\sigma/2$-$\Delta\varepsilon^p/2$ curve.

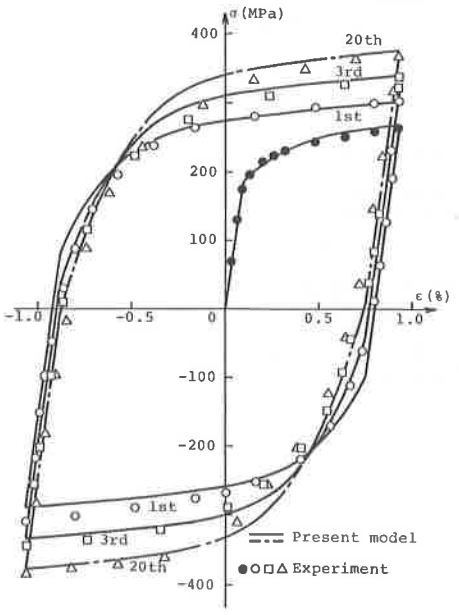

Fig. 4 Stress-strain hysteresis loop of constant strain-range ($\Delta\varepsilon$ = 1.996 %, R_ε = -1.14).

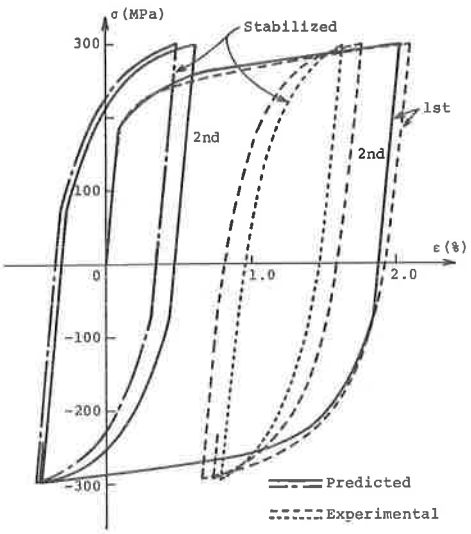

Fig. 5 Stress-strain hysteresis loop of constant stress-range ($\Delta\sigma$ = 594. 0 MPa, R_σ = -1.0).

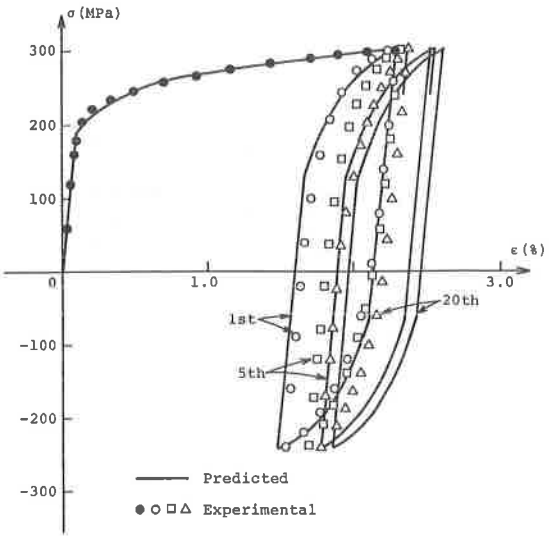

Fig. 6 Stress-strain hysteresis loop of constant stress-range ($\Delta\sigma$ = 546.1 MPa, R_σ = -0.8).

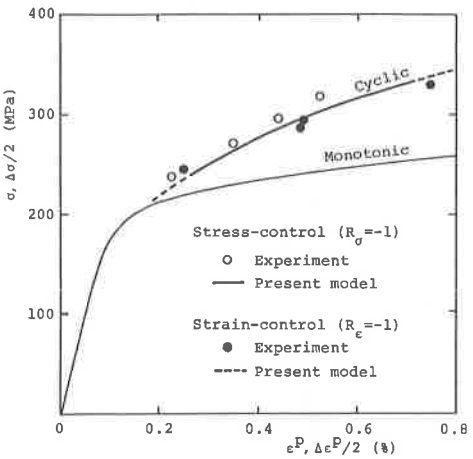

Fig. 7 Comparison between cyclic stress-strain curves under stress- and strain-controlled cyclic loadings.